Supporting information

Genetic targeting of solvatochromic dyes for probing nanoscale environment of proteins in organelles

Rémi Pelletier,[1, #] Dmytro I. Danylchuk,[1, #] Hela Benaissa,[2] Fanny Broch,[2] Romain Vauchelles,[1] Arnaud Gautier,[2] Andrey S. Klymchenko[1,*]

[1] Laboratoire de Bioimagerie et Pathologies, UMR 7021 CNRS, Université de Strasbourg, 74 route du Rhin, 67401, Illkirch, France

[2] Sorbonne Université, École Normale Supérieure, Université PSL, CNRS, Laboratoire des Biomolécules, LBM, 75005 Paris, France.

[#] These authors contributed equally.

* Corresponding author: andrey.klymchenko@unistra.fr

Table of Content

Experimental information

General Methods and Materials. All the reagents were purchased from Sigma-Aldrich, Alfa Aesar, or TCI and used as received. Milli-Q-water (Millipore) was used in all experiments. NMR spectra were recorded at 20 °C on a Bruker Avance III 400 spectrometer. Mass spectra were obtained using an Agilent Q-TOF 6520 mass spectrometer. Absorption spectra were recorded on a Cary 5000-UV-Vis-NIR spectrophotometer (Agilent), and emission spectra were recorded on a FS5 (Edinburgh Instruments) spectrofluorometer. NR probes titrations with liposomes have been done using a TECAN Spark fluorescence plate reader in black flat-bottomed PS 96-wells plates without lid. NR12A was synthesized according to the previously published procedure.

Preparation of Liposomes. All types of large unilamellar vesicles (LUVs) used were prepared by the following procedure. A stock solution of corresponding lipid(s) in chloroform was placed into a round-neck flask, after which the solvent was evaporated in vacuo and phosphate buffer (20 mM, pH 7.4) was added. After all of the solid had dissolved, a suspension of multilamellar vesicles was extruded by using a Lipex Biomembranes extruder (Vancouver, Canada). The size of the filters was first 0.2 μm (7 passages) and thereafter 0.1 μm (10 passages). This generates monodisperse LUVs with a mean diameter of 0.12 μm, as measured with a Malvern Zetamaster 300 (Malvern, U.K.).

Cell Lines, Culture Conditions, and Treatment. KB (ATCC CCL-17) cells were grown in Dulbecco's modified eagle medium (DMEM, Gibco Invitrogen) and supplemented with 10% fetal bovine serum (FBS, Lonza), 1% L-glutamine (Sigma-Aldrich), 1% non-essential amino acid solution (Gibco-Invitrogen), and 1% MEM vitamin solution (Gibco-Invitrogen) at 37 °C in a humidified 5% CO2 atmosphere. Cells were seeded onto a chambered coverglass (IBIDI) at a density of 5×10^4 cells/well. Cells were seeded 24 h before the microscopy measurement for **NR12A** probe. For Halo-NR, cells have been imaged 24 h after transfection. For microscopy imaging with **NR12A**, the attached cells in IBIDI dishes were washed once with warm Hanks' balanced salt solution (HBSS, Gibco-Invitrogen); after that, 1 mL of a corresponding dye solution in warm HBSS was added and the cells were incubated for 10 min at room temperature. For HaloTag probes, cells in IBIDI dishes were washed once with warm phosphate buffer saline (PBS, Gibco-Invitrogen), after that, 1 mL of a corresponding dye solution in warm Opti-MEM was added and the cells were incubated for 30 min at 37 °C. Then, the staining solution was washed and attached cells were incubated in complete medium for 30 min at 37 °C under 5% CO_2 atmosphere to remove unreacted dye. Before imaging, attached cells were always washed with Opti-MEM once and microscopy experiments were run in Opti-MEM.

Transfection: KB cells have been transfected 24 h after being seeded in Ibidi chambers. Transfection mix have been prepared by preparing extemporaneously solution A containing lipofectamine 2000 (4 μL, invitrogen) in warmed Opti-MEM (100 μL) and solution B of pDNA (1.6 μg) in warmed Opti-MEM (100 μL). After 5 min at room temperature, solutions A and B were mixed thoroughly and stayed 20 min at room temperature. Cells were washed with warmed PBS once and placed in 1 mL of warmed Opti-MEM. Transfection mix was added on cells that were gently swirled to ensure even distribution. Cells were incubated at 37 °C for 6 h. Then, transfection media was removed and cells were washed with complete growing media twice and incubated at 37 °C under 5% CO_2 atm for 24 h before imaging.

Unsaturated lipid diet. For **NR12A** imaging, 16 h to 24 h after been seeded into Ibidi chambers, KB cells have been incubated in growing media supplemented with docosahexaenoic acid (DHA) (20 μM). After 24 h of diet, KB cells have been washed with HBSS and incubated in HBSS with **NR12A** (1 μM) for 10 min. Then, cells were washed with warmed HBSS twice and imaged in Opti-MEM. For

NR12-Halo, 16 h after transfection, KB cells have been incubated in growing media supplemented with docosahexaenoic acid (DHA) (20 µM). After 24 h of diet, KB cells have been labeled as previously described.

Fluorescence Microscopy. Cellular imaging was performed using a Nikon Ti-E inverted microscope, equipped with CFI Plan Apo ×60 oil (NA = 1.4) objective, X-Light spinning disk module (CREST Optics), and a Hamamatsu Orca Flash 4 sCMOS camera with a bandpass filter of 531/40 nm (Semrock) or 600/50 nm (Semrock). The excitation in confocal mode was provided by a 488 or 532 nm diode laser (OXXIUS). The exposure time in confocal mode was set to 500 ms per image frame. All the images were recorded using NIS Elements and then processed using ImageJ software. Ratiometric confocal imaging (CLSM) of KB cells was performed on a Leica TSC SPE confocal microscope with HXC PL APO 63×/ 1.40 OIL CS objective. The excitation light was provided by a 10 mW 488 nm laser, while the fluorescence was detected at two spectral ranges: 550−600 nm ($I_{550-600}$) and 600−650 nm ($I_{600-650}$) in sequential mode by rapid switching to minimize drift; a sum of 20 images is shown. All the parameters at each channel were left constant; the illumination power was adjusted to achieve a good signal for each probe. The laser power settings were at 70% of max intensity. The ratiometric images were generated by using special macros under ImageJ that divides the image of the $I_{550-600}$ channel by that of the $I_{600-650}$ channel. For each pixel, a pseudocolor scale was used for coding the ratio, while the intensity is defined by the integral intensity recorded for both channels at the corresponding pixel. Hyperosmotic stress was induced by replacing half of the cell medium with a 1 M sucrose solution immediately followed by imaging and hypoosmotic stress was induced by replacing the cell medium with sterile water immediately followed by imaging.

Images analysis. Images acquired were processed with ImageJ.[1] Colocalization analysis was performed with JACOP plugin[2] for Pearson's and Mander's coefficients calculation and ratiometry analysis was performed using RatioloJ distributed by PIQ-QuESt platform https://piq.unistra.fr/ from University of Strasbourg.

Molecular Biology. Synthetic oligonucleotides used for cloning were purchased from Integrated DNA Technology. PCR reactions were performed with Q5 polymerase (New England Biolabs) in the buffer provided. PCR products were purified using QIAquick PCR purification kit (Qiagen). Isothermal assemblies (Gibson assembly) were performed using homemade mix prepared according to previously described protocols (modified from the original described protocol). (Gibson Nat Meth 2009) Gibson products were purified using MinElute PCR purification kit (Qiagen). Gibson products were transformed in DH10 E. coli. Small-scale isolation of plasmid DNA was done using QIAprep miniprep kit (Qiagen) from 3 mL of overnight culture supplemented with appropriate antibiotics. Large-scale isolation of plasmid DNA was done using the QIAprep maxiprep kit (Qiagen) from 150 mL of overnight culture supplemented with appropriate antibiotics. All plasmid sequences were confirmed by Sanger sequencing with appropriate sequencing primers (GATC Biotech). The plasmids pAG841, encoding HaloTag fused to the platelet derived growth factor receptor (PDGFR) transmembrane domain (for cell-surface labeling 1), pAG846, encoding HaloTag fused to an endoplasmic reticulum (ER) targeting sequence (for ER labeling), pAG847, encoding HaloTag fused to the N-terminal 81 amino acids of the human beta-1,4- galactosyltransferase for Golgi targeting (for Golgi labeling), pAG848, encoding Halotag fused to zebrafish H2B (for chromatin labeling), pAG849, encoding Halotag fused to microtubule-associated protein (MAP) 4 (for microtubule labeling), pAG850, encoding HaloTag fused to the actin binding peptide LifeAct (for actin labeling) were previously described.[3]

The plasmid pAG842, encoding HaloTag fused to the platelet derived growth factor receptor (PDGFR) transmembrane domain (for cell-surface labeling 2), was constructed by Gibson assembly from the pDisplay vector (Life Technology). The plasmid backbone was amplified by PCR using primers ag571/ag313 and ag853/ag314. The insert coding for HaloTag was amplified by PCR using the primers ag1301/ag1303. The three fragments were then assembled by Gibson assembly.

The plasmid pAG843, encoding HaloTag (for cytosol labeling), was constructed by Gibson assembly from the pIRES vector. The plasmid backbone was amplified by PCR using primers ag358/ag313 and ag311/ag314. The insert coding for HaloTag was amplified by PCR using the primers ag1300/ag1291. The three fragments were then assembled by Gibson assembly.

The plasmid pAG844, encoding HaloTag fused to the inner membrane targeting sequence lyn 11 (for inner membrane labeling) was constructed by Gibson assembly from the plasmid pAG106.[4] The plasmid backbone was amplified by PCR using primers ag313/ag555 and ag311/ag314. The insert coding for HaloTag was amplified by PCR using the primers ag1290/ag1291. The three fragments were then assembled by Gibson assembly.

Table S1. Primers used in this study

primer	sequence
ag311	aaagcttatttctgaagaggacttgtaataggcggccgcgactctagatcataatc
ag313	ctcaccttgctcctgccgagaaagtatcca
ag314	tggatactttctcggcaggagcaaggtgag
ag358	ggtggcagatctgagtccggtag
ag555	gagtccttgcccttggacttgatg
ag571	gtcgacgaacaaaaactcatctcag
ag853	gatgagtttttgttcgtcgacggaaagggctttcttcatgtgc
ag1290	catcaagtccaagggcaaggactccgccggcggcggctccatggcagaaatcggtactggct
ag1291	gtcctcttcagaaataagcttttgttcggatccgccggaaatctcgagcgtcg
ag1300	ccggactcagatctgccaccatggcagaaatcggtactggct
ag1301	gatgagtttttgttcgtcgacgccggaaatctcgagcgtcg
ag1303	gttccactggtgacagatctatggcagaaatcggtactggct

Synthesis and characterization of probes

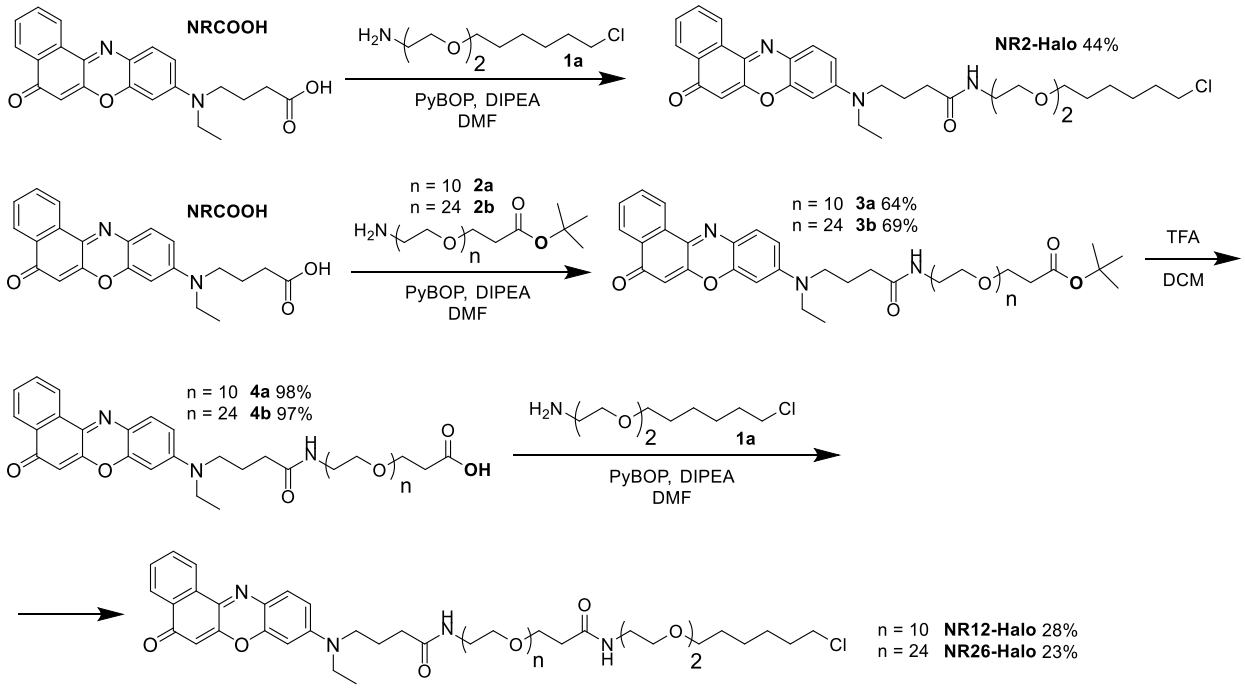

Figure S1. Synthesis of **NR2-Halo**, **NR12-Halo** and **NR26-Halo** from NRCOOH.

Previously reported compounds have been synthetized as described:
Nile Red acid (compound **NRCOOH**)[5] and HaloTag amine (compound **1a**).[6]

Nile Red HaloTag (**NR2-Halo**)

35 mg of compound **NRCOOH** were dissolved in 1 ml of dry DMF together with 36 mg (48 L, 3 eq.) of DIPEA under Ar atmosphere. After 5 minutes, a solution of 50.9 mg (1.05 eq.) of PyBOP 1 ml of dry DMF was added and the mixture was stirred for 30 min at 0 °C. Then, a solution of 40 mg (1.27 eq.) of amine **1a** in 1 mL of dry DMF was added and the final mixture was left stirring in a cooling bath overnight to gradually heat to r.t. (control by TLC).

After the reaction the solvent was evaporated *in vacuo*, the residue was dissolved in EtOAc, washed with citric acid (5%$_{aq}$), H_2O and brine, dried over Na_2SO_4 and filtered, then the solvent was evaporated *in vacuo*.

The crude product was purified by excusive column chromatography (LH-20; DCM:MeOH 1:1), followed by two consecutive runs of preparative TLC (SiO_2; DCM:MeOH 92:8, then SiO_2; EtOAc:MeOH 95:5). Yield: 24 mg (44 %) as a dark red solid. **^{1}H NMR (400 MHz, $CDCl_3$) δ ppm** 8.63 (d, *J*=8.3 Hz, 1 H) 8.28 (dd, *J*=7.8, 1.3 Hz, 1 H) 7.71 (td, *J*=7.5, 1.2 Hz, 1 H) 7.64 (td, *J*=7.3, 1.3 Hz, 1 H) 7.57 (d, *J*=9.0 Hz, 1 H) 6.69 (dd, *J*=9.0, 2.5 Hz, 1 H) 6.49 (d, *J*=2.5 Hz, 1 H) 6.36 (s, 1 H) 6.11 - 6.18 (m, 1 H) 3.40 - 3.63 (m, 16 H) 2.27 (t, *J*=6.9 Hz, 2 H) 1.99 (quin, *J*=7.3 Hz, 2 H) 1.75 (quin, *J*=7.1 Hz, 2 H) 1.58 (quin, *J*=7.1 Hz, 2 H) 1.39 - 1.48 (m, 2 H) 1.35 (m, *J*=6.8 Hz, 2 H) 1.24 (t, *J*=7.0 Hz, 3 H). **^{13}C NMR (101 MHz, DMSO-d_6) δ ppm** 183.70 ($C_{carbonyl}$) 171.76 (C_{amide}) 152.09 (C_{ar}) 150.94 (C_{ar}) 146.65 (C_{ar}) 140.07 (C_{ar}) 132.04 (C_{ar}) 131.72 (C_{ar}) 131.29 (C_{ar}) 131.10 (C_{ar}) 129.91 (C_{ar}) 125.64 (C_{ar}) 125.02 (C_{ar}) 123.79 (C_{ar}) 109.89 (C_{ar}) 105.72 (C_{ar}) 96.52 (C_{ar}) 71.22 (C_{al}) 70.23 (C_{al}) 69.98 (C_{al}) 69.73 (C_{al}) 49.98 (C_{al}) 45.45 (C_{al}) 44.97 (C_{al}) 39.24 (C_{al}) 32.95 (C_{al}) 32.47 (C_{al}) 29.41 (C_{al}) 26.63 (C_{al}) 25.37 (C_{al}) 23.04 (C_{al}) 12.33 (CH_3). **HRMS (ESI), *m/z*:** $[M+Na]^+$ calcd for $C_{32}H_{40}ClN_3O_5Na$, 604.2554; found, 604.2531.

Nile Red PEG t-Bu ester general procedure (**3a and 3b**)

100 mg of compound **NRCOOH** were dissolved in 2 ml of dry DMF together with 103.6 mg (139 µL, 3 eq.) of DIPEA under Ar atmosphere. After 5 minutes, a solution of 145.3 mg (1.05 eq.) of PyBOP 2 ml of dry DMF was added and the mixture was stirred for 30 min at 0 °C. Then, a solution of (1.05 eq.) of a corresponding amine (**2a** or **2b**) in 2 mL of dry DMF was added and the final mixture was left stirring in a cooling bath overnight to gradually heat to r.t. (control by TLC).
After the reaction the solvent was evaporated *in vacuo*. The crude product was purified by excusive column chromatography (LH-20; DCM:MeOH 1:1), followed by gradient column chromatography (SiO_2; DCM:MeOH 99:1 to 97:3 for compound **3a** and SiO_2; DCM:MeOH 99:1 to 8:2 for compound **3b**).
Compound **3a**: yield 160 mg (64 %) as a dark red oil. **^{1}H NMR (400 MHz, $CDCl_3$) δ ppm** 8.64 (dd, *J*=8.2, 1.1 Hz, 1 H) 8.29 (dd, *J*=7.8, 1.5 Hz, 1 H) 7.71 (td, *J*=7.5, 1.7 Hz, 1 H) 7.64 (td, *J*=7.5, 1.3 Hz, 1 H) 7.60 (d, *J*=9.0 Hz, 1 H) 6.72 (dd, *J*=9.2, 2.6 Hz, 1 H) 6.52 (d, *J*=2.8 Hz, 1 H) 6.44 (br t, *J*=5.1 Hz, 1 H) 6.38 (s, 1 H) 3.69 (t, *J*=6.5 Hz, 2 H) 3.56 - 3.65 (m, 36 H) 3.42 - 3.52 (m, 6 H) 2.49 (t, *J*=6.5 Hz, 2 H) 2.29 (t, *J*=7.0 Hz, 2 H) 1.95 - 2.04 (m, 4 H) 1.41 - 1.46 (m, 9 H) 1.24 (t, *J*=7.2 Hz, 3 H). **^{13}C NMR (101 MHz, $CDCl_3$) δ ppm** 183.72 ($C_{carbonyl}$) 171.98 (C_{amide}) 170.88 (C_{carbox}) 152.12 (C_{ar}) 150.97 (C_{ar}) 146.69 (C_{ar}) 140.05 (C_{ar}) 132.05 (C_{ar}) 131.73 (C_{ar}) 131.29 (C_{ar}) 131.12 (C_{ar}) 129.91 (C_{ar}) 125.66 (C_{ar}) 125.01 (C_{ar}) 123.77 (C_{ar}) 109.92 (C_{ar}) 105.73 (C_{ar}) 96.53 (C_{ar}) 80.49 (C_{al}) 70.53 (C_{al}) 70.51 (C_{al}) 70.50 (C_{al}) 70.49 (C_{al}) 70.47 (C_{al}) 70.45 (C_{al}) 70.31 (C_{al}) 66.87 (C_{al}) 50.05 (C_{al}) 45.46 (C_{al}) 39.26 (C_{al}) 36.24 (C_{al}) 32.81 (C_{al}) 28.08 (C_{al}) 23.04 (C_{al}) 12.34 (CH_3). **HRMS (ESI), *m/z*:** $[M+Na]^+$ calcd for $C_{49}H_{73}N_3O_{15}Na$, 966.4931; found, 966.4921. Compound **3b**: yield 285 mg (69 %) as a dark red oil. **^{1}H NMR (400 MHz, $CDCl_3$) δ ppm** 8.65 (dd, *J*=8.0, 0.8 Hz, 1 H) 8.29 (dd, *J*=7.5, 1.3 Hz, 1 H) 7.71 (td, *J*=7.7, 1.5 Hz, 1 H) 7.65 (dd, *J*=7.8, 1.3 Hz, 1 H) 7.61 (d, *J*=9.0 Hz, 1 H) 6.73 (dd, *J*=9.2, 2.6 Hz, 1 H) 6.53 - 6.56 (m, 1 H) 6.52 (d, *J*=2.8 Hz, 1 H) 6.38 (s, 1 H) 3.69 (t, *J*=6.5 Hz, 2 H) 3.59 - 3.67 (m, 90 H) 3.57 (t, *J*=5.0 Hz, 4 H) 3.41 - 3.52 (m, 6 H) 2.49 (t, *J*=6.5 Hz, 2 H) 2.29 (t, *J*=7.0 Hz, 2 H) 1.98 (quin, *J*=7.4 Hz, 2 H) 1.43 (s, 9 H) 1.24 (t, *J*=7.2 Hz, 3 H). **^{13}C NMR (101 MHz, $CDCl_3$) δ ppm** 183.74 ($C_{carbonyl}$) 172.13 (C_{amide}) 170.92 (C_{carbox}) 152.17 (C_{ar}) 151.04 (C_{ar}) 146.73 (C_{ar}) 140.02 (C_{ar}) 132.09 (C_{ar}) 131.76 (C_{ar}) 131.32 (C_{ar}) 131.15 (C_{ar}) 129.92 (C_{ar}) 125.68 (C_{ar}) 125.04 (C_{ar}) 123.79 (C_{ar}) 109.99 (C_{ar}) 105.73 (C_{ar}) 96.54 (C_{ar}) 80.52 (C_{al}) 70.53 (C_{al}) 70.51 (C_{al}) 70.50 (C_{al}) 70.48 (C_{al}) 70.44 (C_{al}) 70.39 (C_{al}) 70.37 (C_{al}) 70.32 (C_{al}) 70.12 (C_{al}) 69.89 (C_{al}) 66.89 (C_{al}) 50.09 (C_{al}) 45.49 (C_{al}) 39.26 (C_{al}) 36.27 (C_{al}) 32.82 (C_{al}) 28.10 (C_{al}) 23.08 (C_{al}) 12.37 (CH_3). **HRMS (ESI), *m/z*:** $[M+Na]^+$ calcd for $C_{77}H_{129}N_3O_{29}Na$, 1582.8609; found, 1582.8754.

Nile Red PEG carboxylic acid general procedure (**4a and 4b**)
140 mg of compound **3a** or 265 mg of compound **3b** were dissolved in 2 ml of dry CH_2Cl_2, then 2 ml of TFA were added and the mixture was stirred for 2h at r.t. (control by TLC).
After the reaction the solvent was evaporated *in vacuo*, then the solid residue was dissolved in acetonitrile and reevaporated *in vacuo* (3 times).
Compound **4a**: yield 129 mg (98 %) as a dark red oil. **^{1}H NMR (400 MHz, Acetone-d_6) δ ppm** 8.62 (dd, *J*=8.0, 0.8 Hz, 1 H) 8.20 (dd, *J*=7.5, 1.3 Hz, 1 H) 7.79 (td, *J*=7.6, 1.4 Hz, 1 H) 7.70 (td, *J*=7.8, 1.3 Hz, 1 H) 7.61 (d, *J*=9.0 Hz, 1 H) 7.51 (br t, *J*=4.9 Hz, 1 H) 6.91 (dd, *J*=9.3, 2.8 Hz, 1 H) 6.70 (d, *J*=2.8 Hz, 1 H) 6.25 (s, 1 H) 3.72 (t, *J*=6.0 Hz, 2 H) 3.51 - 3.68 (m, 42 H) 3.45 (q, *J*=5.3 Hz, 2 H) 2.57 (t, *J*=6.0 Hz, 2 H) 2.37 (t, *J*=7.0 Hz, 2 H) 2.00 (br t, *J*=8.0 Hz, 2 H) 1.25 (t, *J*=7.0 Hz, 3 H). **^{13}C NMR (101 MHz, Acetone-d_6) δ ppm** 183.62 ($C_{carbonyl}$) 174.30 (C_{amide}) 173.86 (C_{carbox}) 153.43 (C_{ar}) 152.79 (C_{ar}) 148.03 (C_{ar}) 140.61 (C_{ar}) 133.48 (C_{ar}) 133.01 (C_{ar}) 132.67 (C_{ar}) 132.34 (C_{ar}) 131.18 (C_{ar}) 126.54 (C_{ar}) 125.99 (C_{ar}) 124.86 (C_{ar}) 111.62 (C_{ar}) 106.21 (C_{ar}) 97.77 (C_{ar}) 71.39 (C_{al}) 71.29 (C_{al}) 71.13 (C_{al}) 71.11 (C_{al}) 71.08 (C_{al}) 71.06 (C_{al}) 71.03 (C_{al}) 71.00 (C_{al}) 70.94 (C_{al}) 70.89 (C_{al}) 70.83 (C_{al}) 70.81 (C_{al}) 70.78 (C_{al}) 70.72 (C_{al}) 70.71 (C_{al}) 68.03 (C_{al}) 67.71 (C_{al}) 51.19 (C_{al}) 46.49 (C_{al}) 40.26 (C_{al}) 35.74 (C_{al}) 33.62 (C_{al}) 24.40 (C_{al}) 13.12 (CH_3).

HRMS (ESI), *m/z*: $[M-H]^-$ calcd for $C_{45}H_{64}N_3O_{15}$, 886.4343; found, 886.4315. Compound **4b**: yield 248 mg (97 %) as a dark red oil. **^{1}H NMR (400 MHz, Acetone-*d*$_6$) δ ppm** 8.64 (dd, *J*=8.0, 0.8 Hz, 1 H) 8.21 (dd, *J*=7.9, 0.9 Hz, 1 H) 7.81 (td, *J*=7.6, 1.4 Hz, 1 H) 7.72 (td, *J*=7.4, 1.3 Hz, 1 H) 7.63 (d, *J*=9.0 Hz, 1 H) 7.40 (br t, *J*=5.5 Hz, 1 H) 6.94 (dd, *J*=9.0, 2.8 Hz, 1 H) 6.73 (d, *J*=2.8 Hz, 1 H) 6.28 (s, 1 H) 3.53 - 3.77 (m, 100 H) 3.44 (q, *J*=4.9 Hz, 2 H) 2.57 (t, *J*=6.2 Hz, 2 H) 2.36 (t, *J*=7.0 Hz, 2 H) 2.00 (br t, *J*=7.8 Hz, 2 H) 1.26 (t, *J*=7.0 Hz, 3 H). **^{13}C NMR (101 MHz, Acetone-*d*$_6$) δ ppm** 183.59 ($C_{carbonyl}$) 173.77 (C_{amide}) 173.62 (C_{carbox}) 153.50 (C_{ar}) 152.89 (C_{ar}) 148.13 (C_{ar}) 140.63 (C_{ar}) 133.54 (C_{ar}) 133.03 (C_{ar}) 132.75 (C_{ar}) 132.43 (C_{ar}) 131.25 (C_{ar}) 126.60 (C_{ar}) 126.12 (C_{ar}) 124.92 (C_{ar}) 111.75 (C_{ar}) 106.23 (C_{ar}) 97.85 (C_{ar}) 71.46 (C_{al}) 71.35 (C_{al}) 71.30 (C_{al}) 71.29 (C_{al}) 71.26 (C_{al}) 71.24 (C_{al}) 71.23 (C_{al}) 71.21 (C_{al}) 71.16 (C_{al}) 71.14 (C_{al}) 71.11 (C_{al}) 71.06 (C_{al}) 71.04 (C_{al}) 71.03 (C_{al}) 71.00 (C_{al}) 68.08 (C_{al}) 67.76 (C_{al}) 51.26 (C_{al}) 46.56 (C_{al}) 40.23 (C_{al}) 35.73 (C_{al}) 33.60 (C_{al}) 24.41 (C_{al}) 13.17 (CH_3). **HRMS (ESI), *m/z*:** $[M+Na]^+$ calcd for $C_{73}H_{121}N_3O_{29}Na$, 1526.7983; found, 1526.8007.

Nile Red PEG HaloTag general procedure (NR12-Halo and NR26-Halo)

Nile Red PEG carboxylic acid (100 mg in case of compound **3a** or 170 mg in case of compound **3b)** was dissolved in 1 ml of dry DMF together with 4 eq. of DIPEA under Ar atmosphere. After 5 minutes, a solution of 1.4 eq. of PyBOP 1 ml of dry DMF was added and the mixture was stirred for 30 min at 0 °C. Then, a solution of 1.4 eq. of amine **1a** in 1 mL of dry DMF was added and the final mixture was left stirring in a cooling bath overnight to gradually heat to r.t.

After the reaction the solvent was evaporated *in vacuo*. The crude product was purified by excusive column chromatography (LH-20; DCM:MeOH 1:1), followed by preparative TLC (SiO_2; DCM:MeOH 9:1 for both compounds) and reverse phase gradient column chromatography (C18-Silica gel, Acetonitrile:H_2O+0.05 % TFA 2:8 to 1:1 (for both compounds).

Compound **NR12-Halo**: yield 35 mg (28 %) as a dark red oil. **^{1}H NMR (400 MHz, $CDCl_3$) δ ppm** δ ppm 8.65 (dd, *J*=8.0, 0.8 Hz, 1 H) 8.30 (dd, *J*=7.9, 0.9 Hz, 1 H) 7.73 (td, *J*=7.6, 1.4 Hz, 1 H) 7.60 - 7.68 (m, 2 H) 7.14 (br t, *J*=4.8 Hz, 1 H) 7.01 (br t, *J*=5.8 Hz, 1 H) 6.78 (dd, *J*=9.0, 2.8 Hz, 1 H) 6.55 (d, *J*=2.8 Hz, 1 H) 6.52 (s, 1 H) 3.72 (t, *J*=5.9 Hz, 2 H) 3.41 - 3.65 (m, 56 H) 2.49 (t, *J*=5.9 Hz, 2 H) 2.33 (t, *J*=7.0 Hz, 2 H) 1.94 - 2.04 (m, 2 H) 1.75 (quin, *J*=6.8 Hz, 2 H) 1.58 (quin, *J*=7.2 Hz, 2 H) 1.39 - 1.48 (m, 2 H) 1.31 - 1.39 (m, 2 H) 1.25 (t, *J*=7.0 Hz, 3 H). **^{13}C NMR (101 MHz, DMSO-*d*$_6$) δ ppm** 183.34 ($C_{carbonyl}$) 172.70 (C_{amide}) 172.23 (C_{amide}) 152.31 (C_{ar}) 151.48 (C_{ar}) 146.89 (C_{ar}) 139.07 (C_{ar}) 132.03 (C_{ar}) 131.52 (C_{ar}) 131.47 (C_{ar}) 131.12 (C_{ar}) 129.89 (C_{ar}) 125.89 (C_{ar}) 125.69 (C_{ar}) 123.80 (C_{ar}) 110.89 (C_{ar}) 104.88 (C_{ar}) 96.48 (C_{ar}) 71.27 (C_{al}) 70.44 (C_{al}) 70.40 (C_{al}) 70.38 (C_{al}) 70.36 (C_{al}) 70.33 (C_{al}) 70.28 (C_{al}) 70.22 (C_{al}) 70.20 (C_{al}) 70.06 (C_{al}) 70.00 (C_{al}) 69.80 (C_{al}) 69.63 (C_{al}) 67.15 (C_{al}) 54.34 (C_{al}) 50.65 (C_{al}) 50.22 (C_{al}) 45.67 (C_{al}) 45.02 (C_{al}) 44.99 (C_{al}) 39.40 (C_{al}) 39.33 (C_{al}) 36.68 (C_{al}) 32.68 (C_{al}) 32.50 (C_{al}) 29.40 (C_{al}) 26.66 (C_{al}) 25.38 (C_{al}) 23.12 (C_{al}) 12.34 (CH_3). **HRMS (ESI), *m/z*:** $[M+Na]^+$ calcd for $C_{55}H_{85}ClN_4O_{16}Na$, 1115.5547; found, 1115.5519.

Compound **NR26-Halo**: yield 45 mg (23 %) as a dark red oil. **^{1}H NMR (400 MHz, $CDCl_3$) δ ppm** 8.68 (dd, *J*=8.0, 0.9 Hz, 1 H) 8.32 (dd, *J*=8.0, 0.8 Hz, 1 H) 7.74 (td, *J*=7.5, 1.4 Hz, 1 H) 7.63 - 7.68 (m, 2 H) 7.07 - 7.14 (m, 1 H) 6.96 - 7.02 (m, 1 H) 6.80 (dd, *J*=9.3, 2.5 Hz, 1 H) 6.57 (d, *J*=2.5 Hz, 1 H) 6.55 (s, 1 H) 3.73 (t, *J*=5.9 Hz, 2 H) 3.42 - 3.67 (m, 112 H) 2.50 (t, *J*=5.9 Hz, 2 H) 2.33 (t, *J*=7.0 Hz, 2 H) 1.99 (br quin, *J*=7.3 Hz, 2 H) 1.76 (quin, *J*=7.1 Hz, 2 H) 1.59 (quin, *J*=7.1 Hz, 2 H) 1.40 - 1.49 (m, 2 H) 1.31 - 1.40 (m, 2 H) 1.25 (t, *J*=7.0 Hz, 3 H). **^{13}C NMR (101 MHz, DMSO-*d*$_6$) δ ppm** 183.31 ($C_{carbonyl}$) 172.74 (C_{amide}) 172.47 (C_{amide}) 152.37 (C_{ar}) 151.56 (C_{ar}) 146.96 (C_{ar}) 139.00 (C_{ar}) 132.04 (C_{ar}) 131.57 (C_{ar}) 131.57 (C_{ar}) 131.04 (C_{ar}) 129.91 (C_{ar}) 126.08 (C_{ar}) 125.75 (C_{ar}) 123.81 (C_{ar}) 111.04 (C_{ar}) 104.78 (C_{ar}) 96.51 (C_{ar})

71.32 (C_{al}) 71.27 (C_{al}) 70.47 (C_{al}) 70.44 (C_{al}) 70.41 (C_{al}) 70.37 (C_{al}) 70.36 (C_{al}) 70.34 (C_{al}) 70.29 (C_{al}) 70.25 (C_{al}) 70.23 (C_{al}) 70.08 (C_{al}) 70.02 (C_{al}) 69.74 (C_{al}) 69.59 (C_{al}) 67.11 (C_{al}) 50.24 (C_{al}) 45.71 (C_{al}) 45.02 (C_{al}) 39.44 (C_{al}) 39.38 (C_{al}) 36.61 (C_{al}) 32.67 (C_{al}) 32.51 (C_{al}) 29.42 (C_{al}) 26.67 (C_{al}) 25.40 (C_{al}) 23.13 (C_{al}) 12.34 (CH_3). **HRMS (ESI), *m/z*:** $[M+2Na]^{+2}$ calcd for $C_{83}H_{141}ClN_4O_{30}Na_2$, 877.4557; found, 877.4522.

MS spectra of synthetized probes

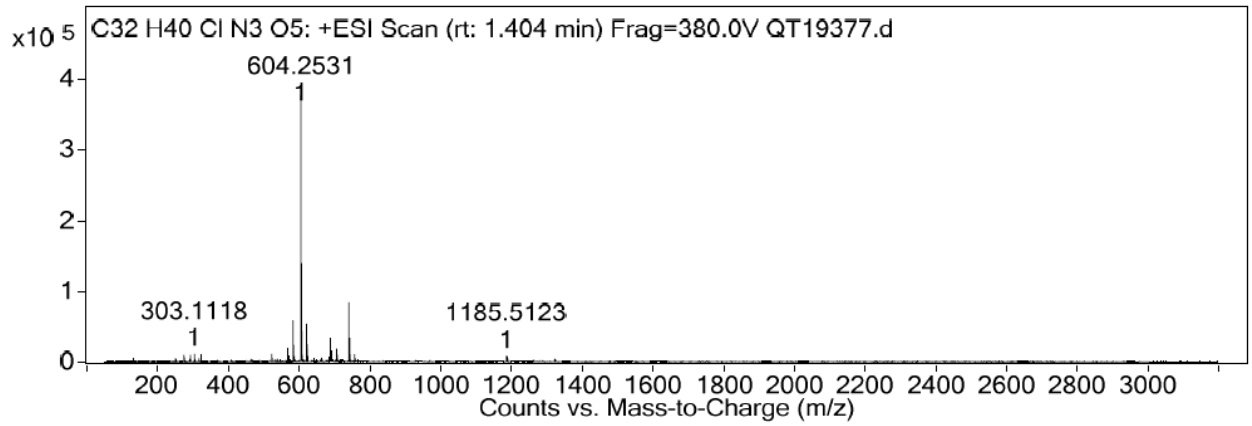

Figure S2. Mass spectra of **NR2-Halo**.

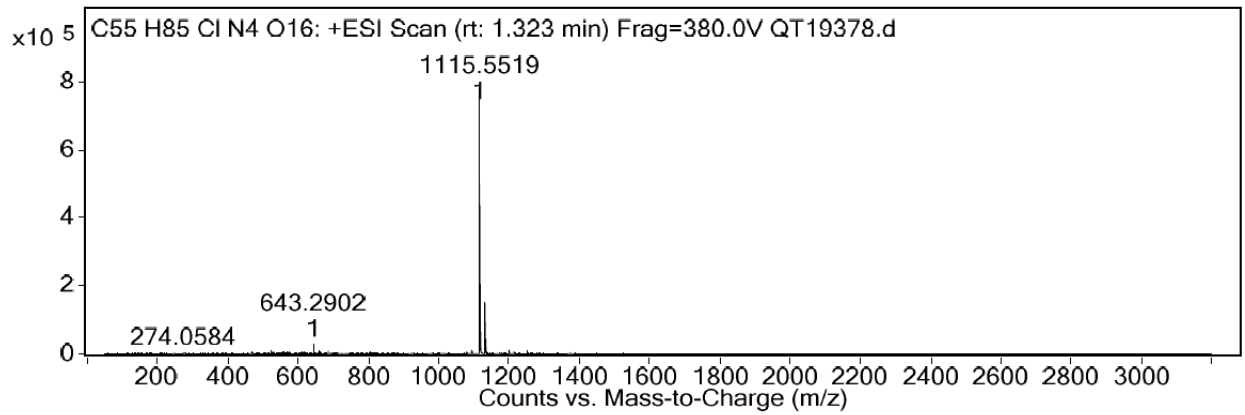

Figure S3. Mass spectra of **NR12-Halo**.

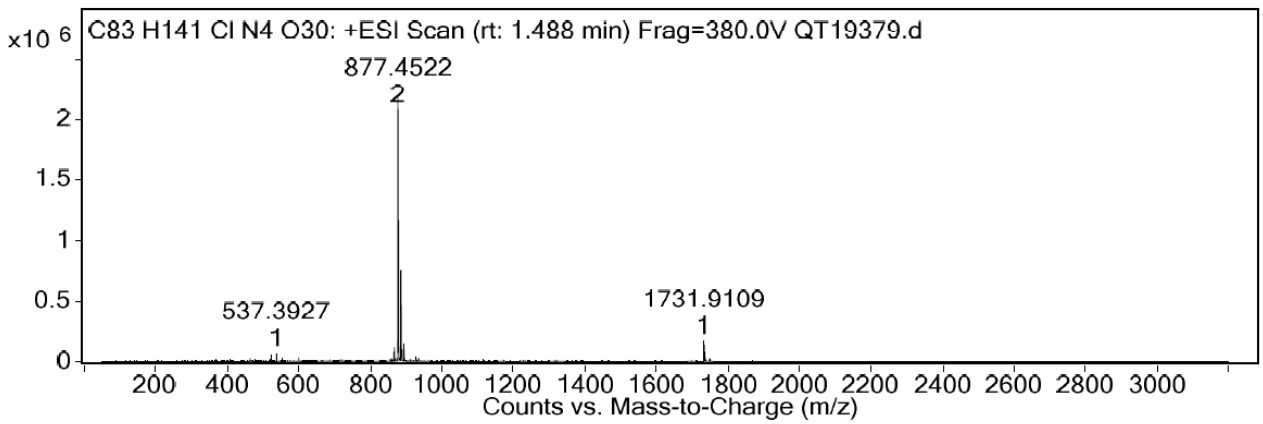

Figure S4. Mass spectra of **NR26-Halo**.

Spectroscopy

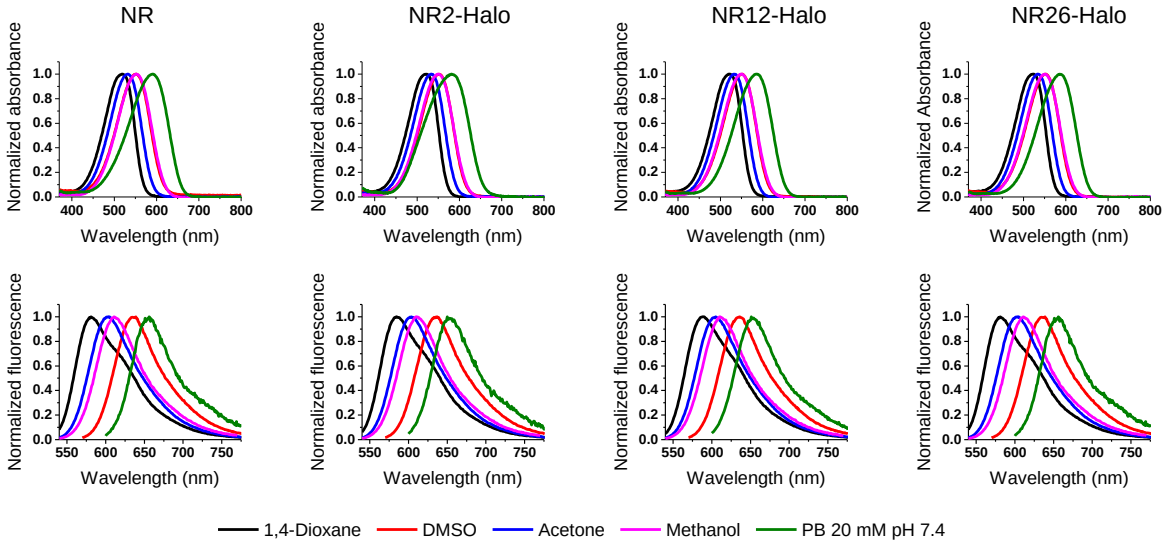

Figure S5. Normalized absorbance and fluorescent spectra of studied NR derivatives in various solvents. Excitation wavelength are respectively 520 nm, 550 nm, 530 nm, 550 nm, 590 nm in 1,4-dioxane, DMSO, acetone, methanol and in phosphate buffer (PB) 20 mM at pH = 7.4.

Microscopy and cellular imaging

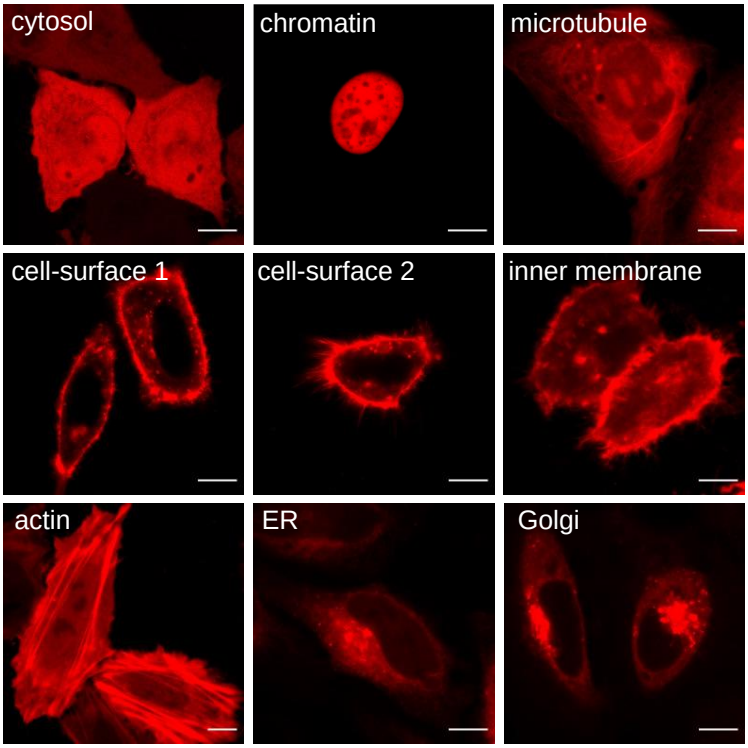

Figure S6. Labeling of HaloTag fusions with TMR-ligand: Halotag (cytosol), H2B-Halotag (chomatin), MAP4-Halotag (microtubule), pDisplay-Halotag (cell surface 1), min(Dis)-Halotag (cell surface 2), lyn11-Halotag (inner membrane), LifeAct-Halotag (actin), ER-Halotag (Endoplasmic reticulum), golgi-Halotag (Golgi apparatus). Scale bars 10 μm.

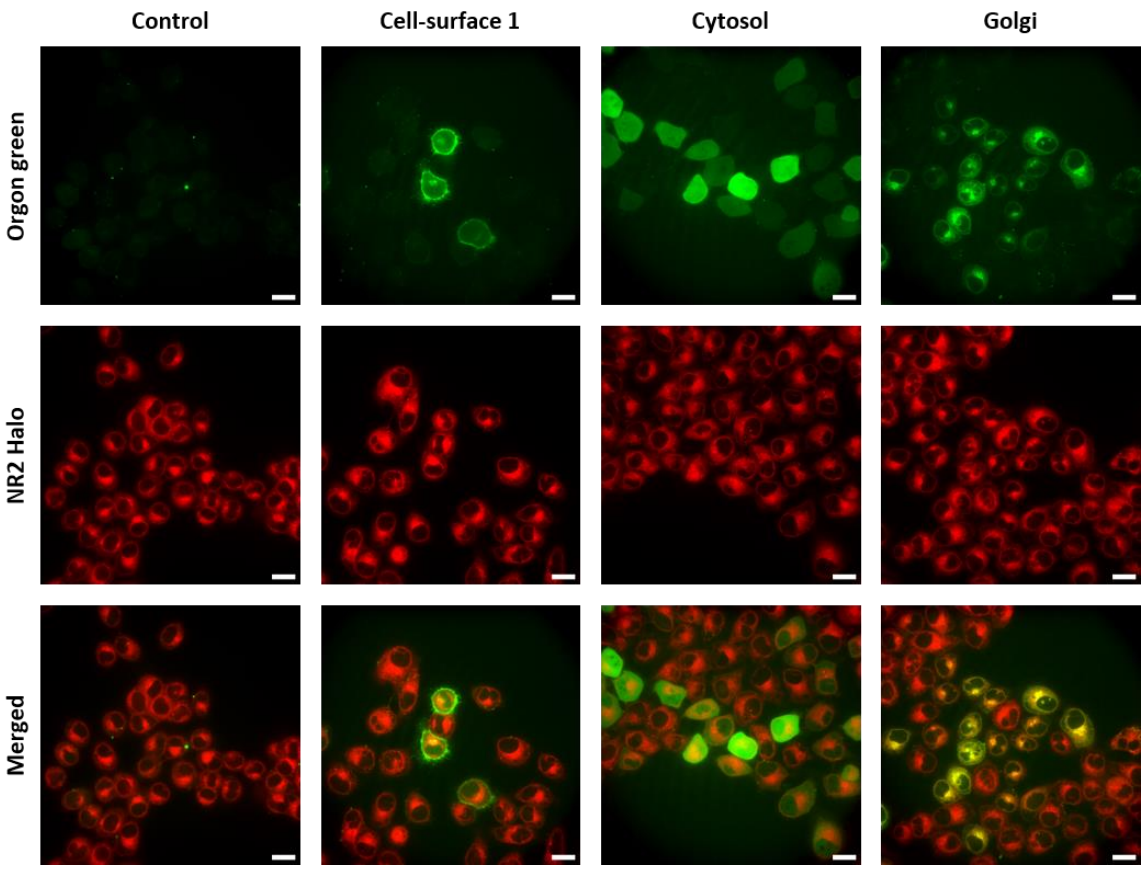

Figure S7. Colocalization of **NR2-Halo** and Oregon Green HaloTag in transfected KB cells in confocal spinning disk microscopy. Transfected cells were incubated in Opti-MEM supplemented with **NR2-Halo** (500 nM) and Oregon Green HaloTag (500 nM) for 30 min at 37 °C. Afterwards, cells were incubated in complete medium for 30 min at 37 °C and finally changed for Opti-MEM before imaging. Scale bars are set at 20 µm.

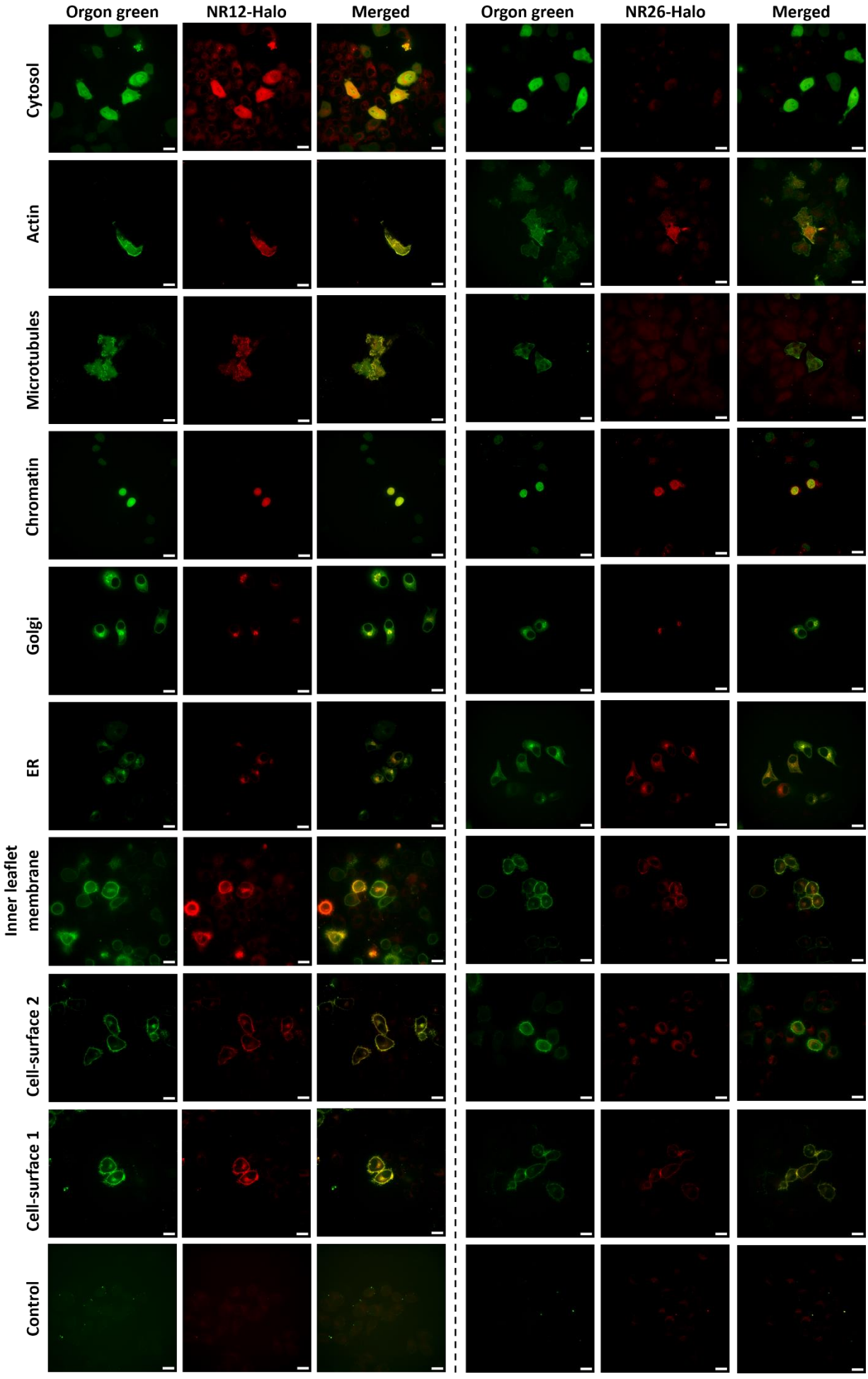
Orgon green
NR12-Halo
Merged
Orgon green
NR26-Halo
Merged
Cytosol
Actin
Microtubules
Chromatin
Golgi
ER
Inner leaflet membrane
Cell-surface 2
Cell-surface 1
Control

Figure S8. Colocalization of **NR12-Halo** and Oregon Green HaloTag in transfected KB cells in confocal spinning disk microscopy. Transfected cells were incubated in Opti-MEM supplemented with **NR12-Halo** or **NR26-Halo** (500 nM) and Oregon Green HaloTag (500 nM) for 30 min at 37 °C. Afterwards, cells were incubated in complete medium for 30 min at 37 °C and finally changed for Opti-MEM before imaging. Scale bars are 20 µm.

Table S2. Pearson's and Mander's coefficients calculated with JACOP[2] plugin for ImageJ[7] for the respective colocalization of **NR12-Halo** and **NR26-Halo** with Oregon Green HaloTag in transfected KB cells (*n* = 3).

HaloTag location	Pearson's		Manders's	
	NR12-Halo	NR26-Halo	NR12-Halo	NR26-Halo
Cell surface	0.756	0.872	M_1 0.974 M_2 0.513	0.987 0.609
Cell surface	0.833	0.571	M_1 0.859 M_2 0.694	0.225 0.835
CMV	0.714	0.509	M_1 0.943 M_2 0.739	0.574 0.548
Inner leaflet	0.708	0.830	M_1 0.511 M_2 0.477	0.998 0.300
Golgi	0.784	0.811	M_1 0.801 M_2 0.719	0.998 0.307
ER	0.857	0.773	M_1 0.978 M_2 0.785	0.994 0.781
Chromatin	0.970	0.637	M_1 0.799 M_2 0.900	0.759 0.481
microtubules	0.820	0.449	M_1 0.719 M_2 0.902	0.234 0.568
Actin	0.769	0.680	M_1 0.925 M_2 0.509	0.470 0.884
Control (no tranfection)	0.465	0.387	M_1 0.042 M_2 0.744	0.249 0.743

Polarity analysis

The following discussion about the ratiometry analysis have been illustrated using a test pattern (Figure S11). It is a dual channel image with five ROI containing the same number of pixel and centered around a Gaussian shape. In each ROI, the sum of all the pixel's intensity in both channel is constant and ROI have been built to give a ratiometric distribution respectively centered on 0.25, 0.5, 1, 2 and 4 from left to right when channel A is divided by channel B.

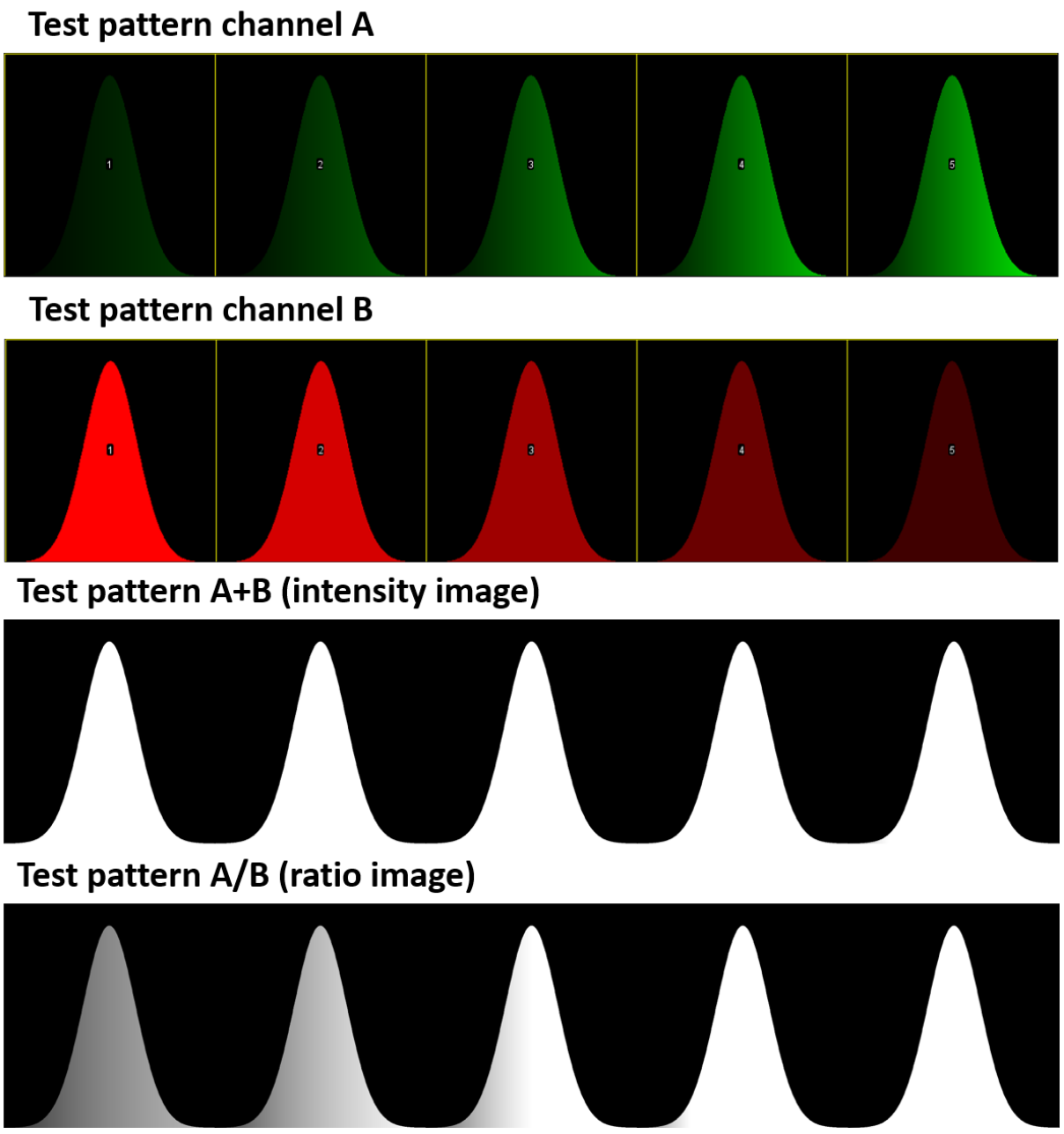

Figure S9. Test pattern used to test the analysis methods. In each five ROI displayed, the number of pixels is the same and the sum of intensity is constant. Each Gaussian shapes have been built to give a respective ratio of 0.25, 0.5, 1, 2 and 4 from left to right when channel A is divided by channel B.

For ratiometric analysis, the ImageJ macro RatioloJ have been used as distributed for ratio analysis and adapted as described below for the polarity index reported. The principle of this

macro has been reported before.[8,9] RatioloJ is an imageJ macro for quality ratiometric imaging. Although ratiometric imaging can be performed by a simple division of two images from different channels, the resulting image presents several drawbacks. First, as the pixels intensities are divided, the information regarding the initial pixels' intensity is lost. Then, the image displays object that are faded in the color-coded background resulting hardly readable image. Herein we developed RatioloJ, a macro running on ImageJ for an enhanced readout of ratiometric imaging. RatioloJ allows to obtain ratiometric images with adjustable scales and enables the creation of distribution curves of ratio to quantify the probe state in selected regions of interest. Principe. To circumvent these aforementioned drawbacks, several processing steps are performed. First, pixels under a user-defined threshold are set to zero without alteration of other pixels in order to create a mask used to subtract the background. Then, in the one hand the channels are summed to make intensity picture and on the other hand the channels are divided to make the ratio picture. Finally, in the ratioloJ image the pixels' intensity is coded by the brightness whereas the pixels'ratio value is color-coded, resulting in a clean and readable ratiometric image. RatioloJ also enables to create histograms of the ratio distribution of the whole picture as well as in defined regions of interest. For each pixel of selected areas, its value in the intensity image is summed to the abscise of the value in the ratio image. The obtained values build up a curve where statistical values like averages and maxima can be extracted from chosen areas. RatioloJ is available for download at this link: https://piq.unistra.fr/analyse-dimages/outilstelechargeables-pour-imagej

However, the ratiometric analysis relies on the multiplicative inverse, which is a non-linear function (figure S11). For this reason, a distribution of value submitted to an inverse function will be strongly distorted as follow: on one side, distributions of low ratio values will be compressed and appear as narrow peaks, on the other side high ratio values distributions will be extremely broaden and flattened. When our test pattern is submitted to a ratiometric analysis (figure S11), it appears clearly that this approach is not suitable the analysis the homogeneity of two distributions, especially when they are centered on very different ratio values. In addition, Inverting the two channels of interest A and B will lead to two different results. (figure S14-A).

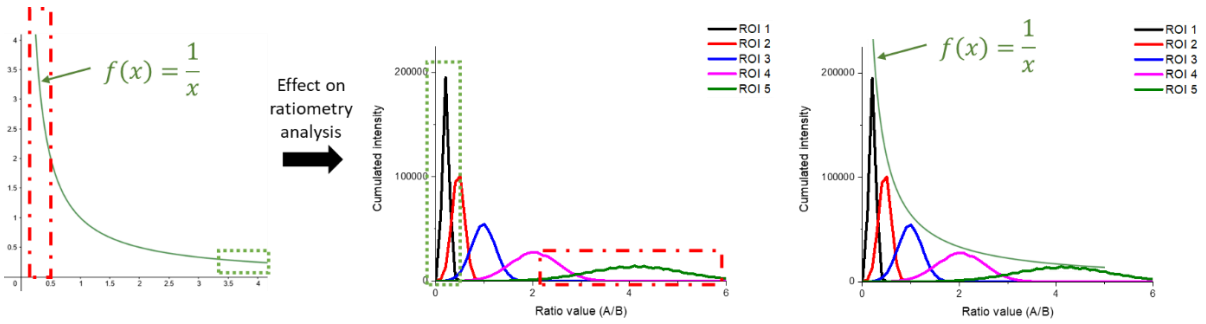

Figure S10. Schematic link between the multiplicative inverse and the ratiometric analysis and its effect on the proposed test pattern.

In the proposed approach, pixels are represented in a Cartesian coordinate plan according to their respective intensity with the two channels of interest as abscissa and ordinates. Then, pixels are sorted regarding their angular coordinate instead of the ratio $\frac{I_{Channel\ A}}{I_{Channel\ B}}$ (figure S13).

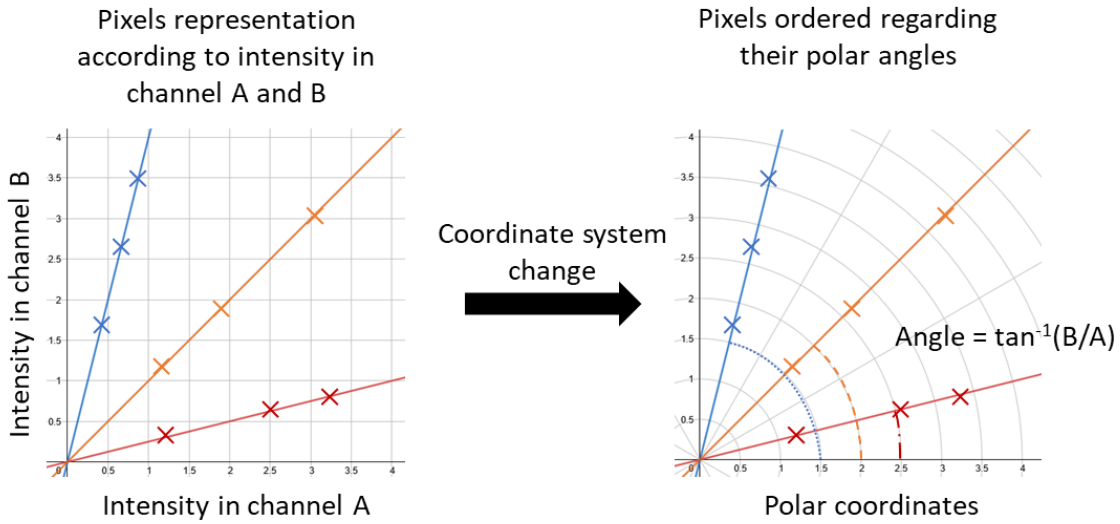

Figure S11. Schematic representation of polar indexation of ratiometric analysis method.

In that way, calculated values are located between 0 (100% of intensity in channel B) and $\frac{\pi}{2} \approx 1.57$ (100% of intensity in channel A). It worth to notice that the angular coordinate can be calculated as $\arctan\left(\frac{I_{Channel\ A}}{I_{Channel\ B}}\right) = \arctan(ratio)$, allowing to easily convert ratiometric results into the present representation. This representation is not free from any distortion as central values around $\frac{\pi}{4}$ (~ 0.785) will be lowered compared to boundary values. But it reduces drastically the crushing effect of the ratio calculation, provides bounded values and restore a symmetry between A vs B and B vs A situations (figure S14-B).

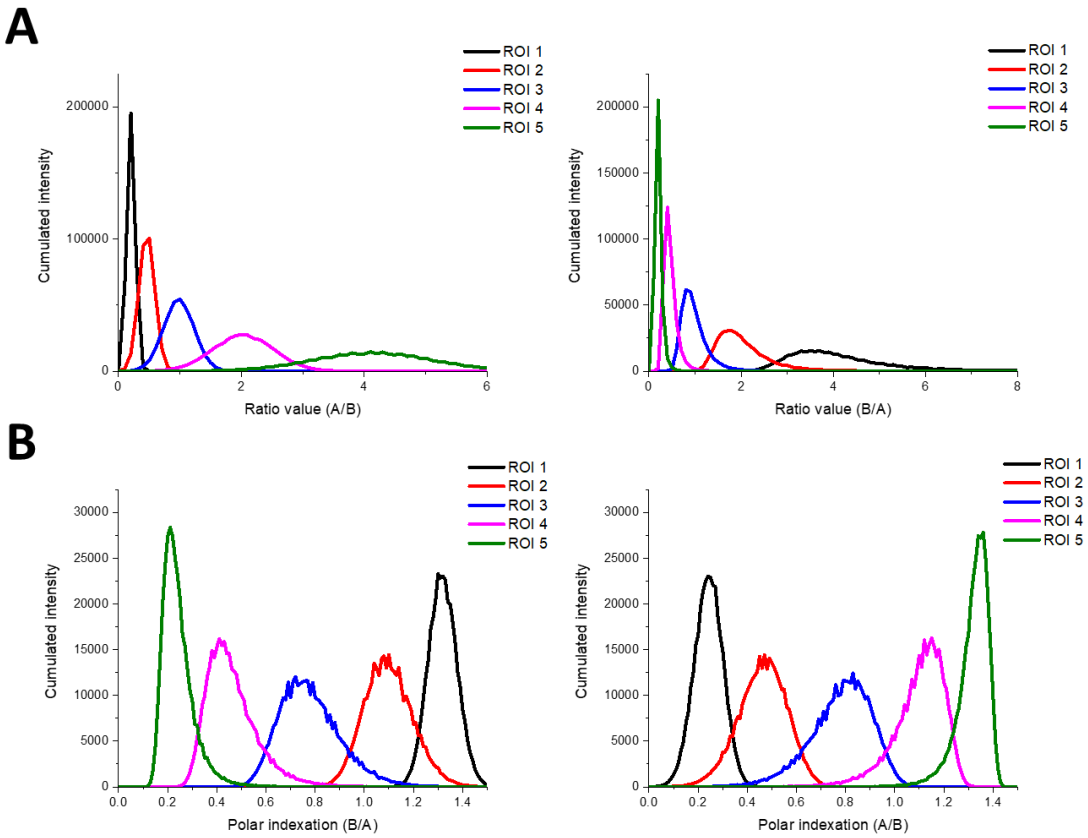

Figure S12. (A) Distributions obtained for each ROI after ratiometric analysis of the test pattern for both A/B case and B/A cases. (B) Distributions obtained for each ROI after polar indexation analysis of the test pattern for both A vs B and B vs A cases.

To facilitate the values interpretations, the $\left[0; \frac{\pi}{2}\right]$ domain will be normalized on the interval $[0; 1]$ in the rest of the study.

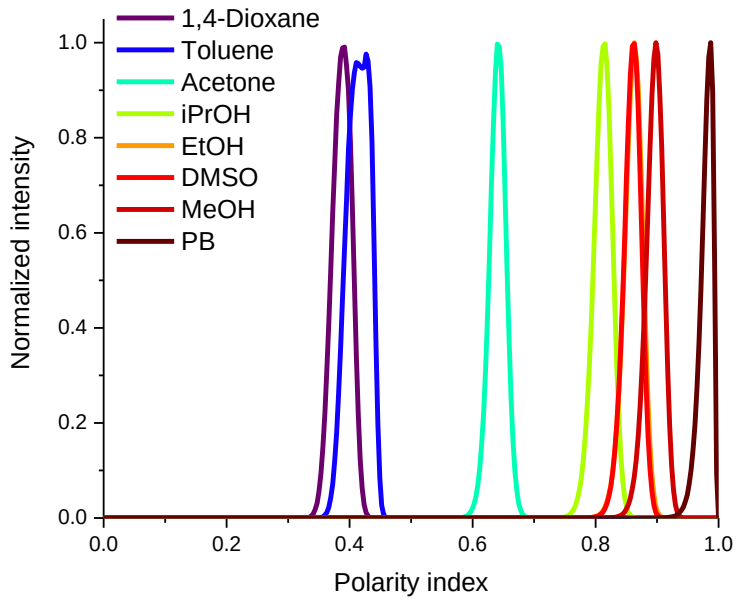

Figure S13. Polarity indexation regarding to various solvents. Solutions of **NR12-Halo** (1 µM) in media of different polarity have been subjected to the same confocal imaging setup and image analysis. The analysis have been performed for channel 600-650 nm vs channel 550-600 nm, in that way, the greater is the value, the greater is the polarity index.

Table S2. Statistic values of distributions obtained from ratiometric analysis for polarity mapping.

Labeling	Mean	Mediane	Quartile 1	Quartile 3
Non transfected control	0.84542	0.785	0.625	1.005
NR12A	1.40891	1.4	1.25	1.56
Cell surface 1	0.48839	0.465	0.39	0.56
Cell surface 2	0.57409	0.54	0.455	0.655
Cytosol	0.26581	0.23	0.175	0.305
Inner membrane leaflet	0.68851	0.66	0.565	0.775
ER	0.46348	0.435	0.365	0.525
Golgi apparatus	0.57386	0.55	0.48	0.64
Chromatin	0.25234	0.19	0.15	0.25
Microtubules	0.39725	0.345	0.275	0.445
Actin	0.28062	0.255	0.19	0.335

Leaflet-specific bleaching

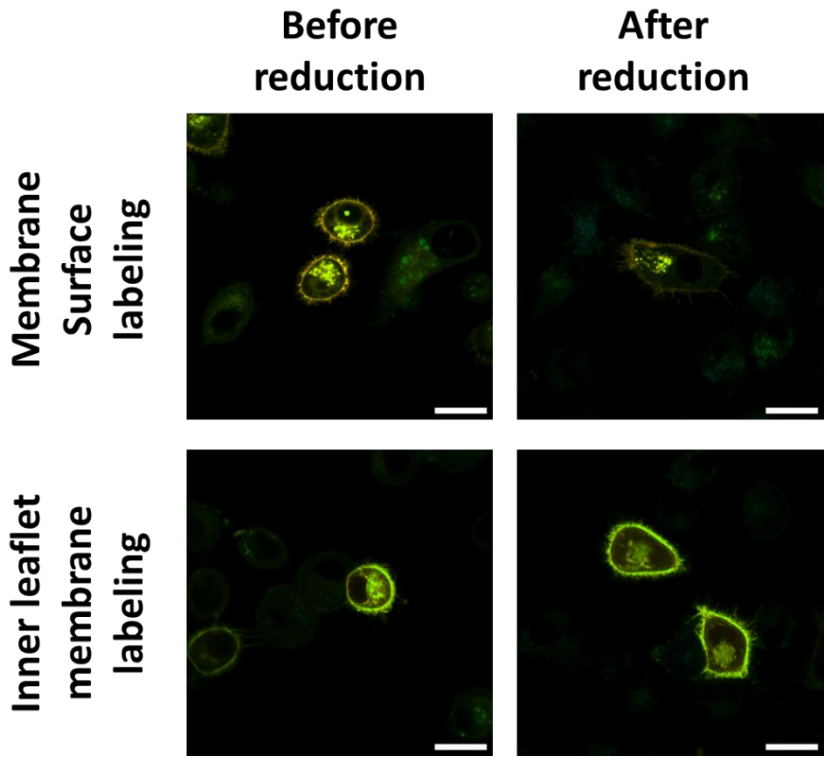

Figure S14. Transfected KB cells expressing HaloTag encoded protein respectively on the cell surface or on the membrane inner leaflet have been imaged by ratiometric CLSM in Opti-MEM using **NR12-Halo** probe before and after reductive bleaching. Accessible **NR12-Halo** compounds bleaching have been performed using sodium dithionite solution at 100 mM for 5 min. Scale bars have been set at 20 µm.

Sodium dithionite treatments induced no visible ratio modification. For the membrane surface labeling, the treatment bleached almost completely all the membrane fluorescence retaining intracellular fluorescence signal. For the inner leaflet labeling, reductive treatment had no visible bleaching effect.

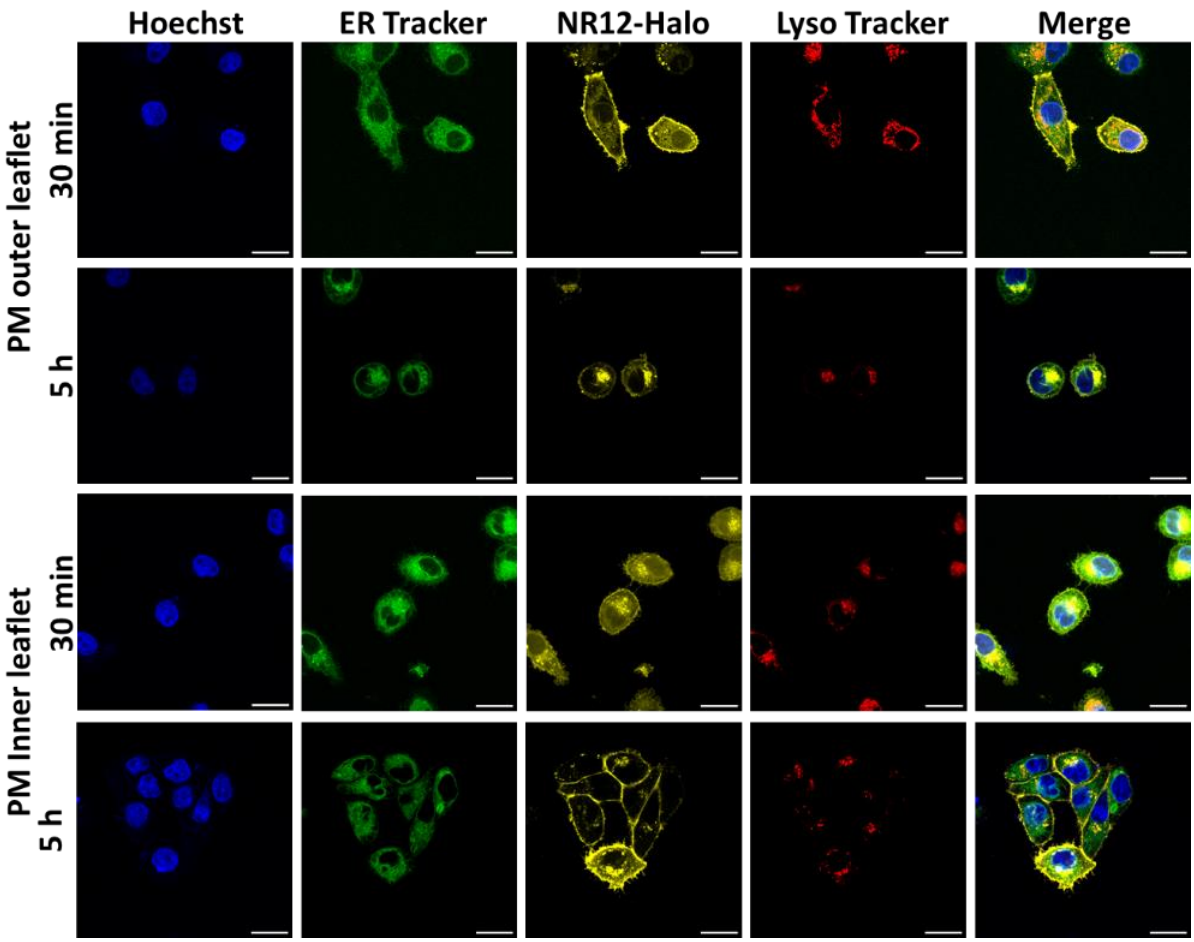

Figure S15. Transfected KB cells expressing HaloTagged proteins on membrane surface 2 and membrane inner leaflet in CLSM at 30 min and 5 h after **NR12-Halo** labelling (30 min incubation with **NR12-Halo** at 1 µM and then washed and incubated in complete growth medium). Nucleus (Hoechst 33258), ER (ER tracker green), lysosomes (Lyso-tracker deep red) have been stained for simultaneous observation. Scale bars: 20 µm.

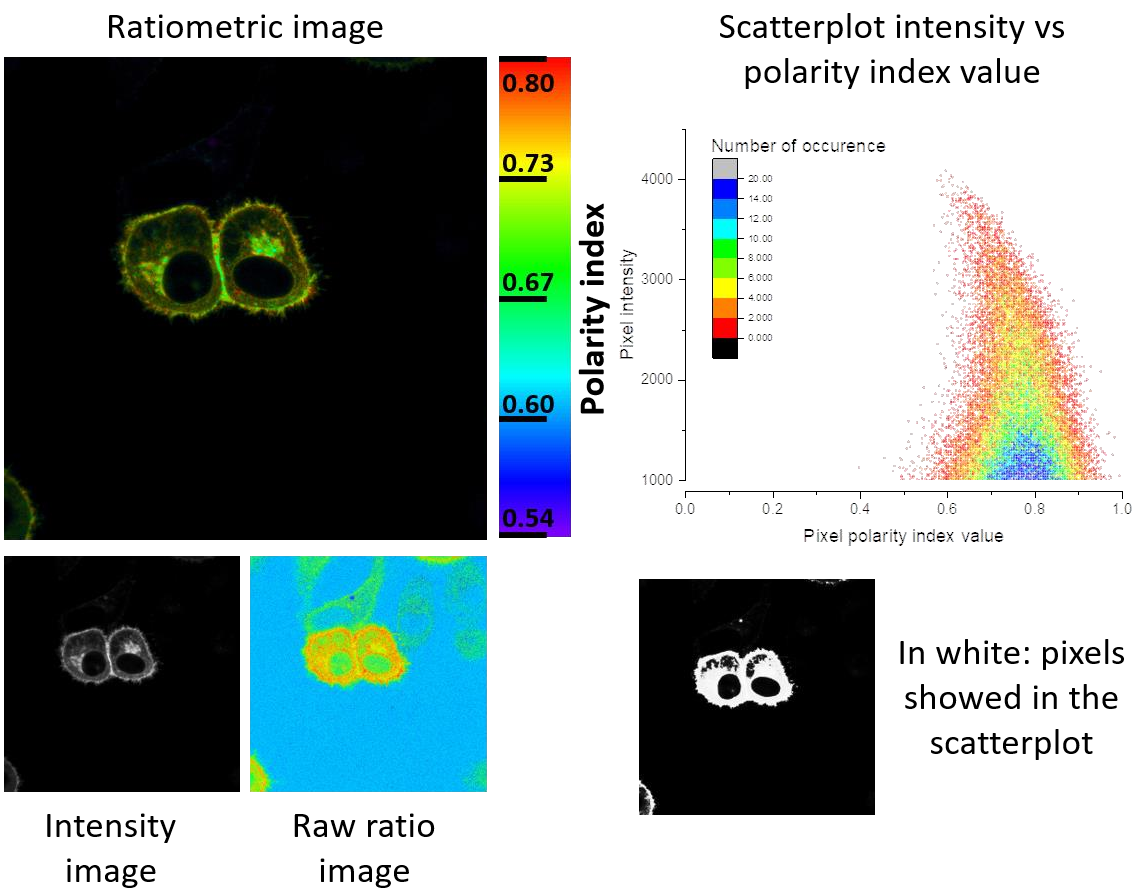

Figure S16. Analysis of the colleration between the polarity index and intensity values for KB cells expressing HaloTagged PM outer leaflet 1 protein labelled with **NR12-Halo**.

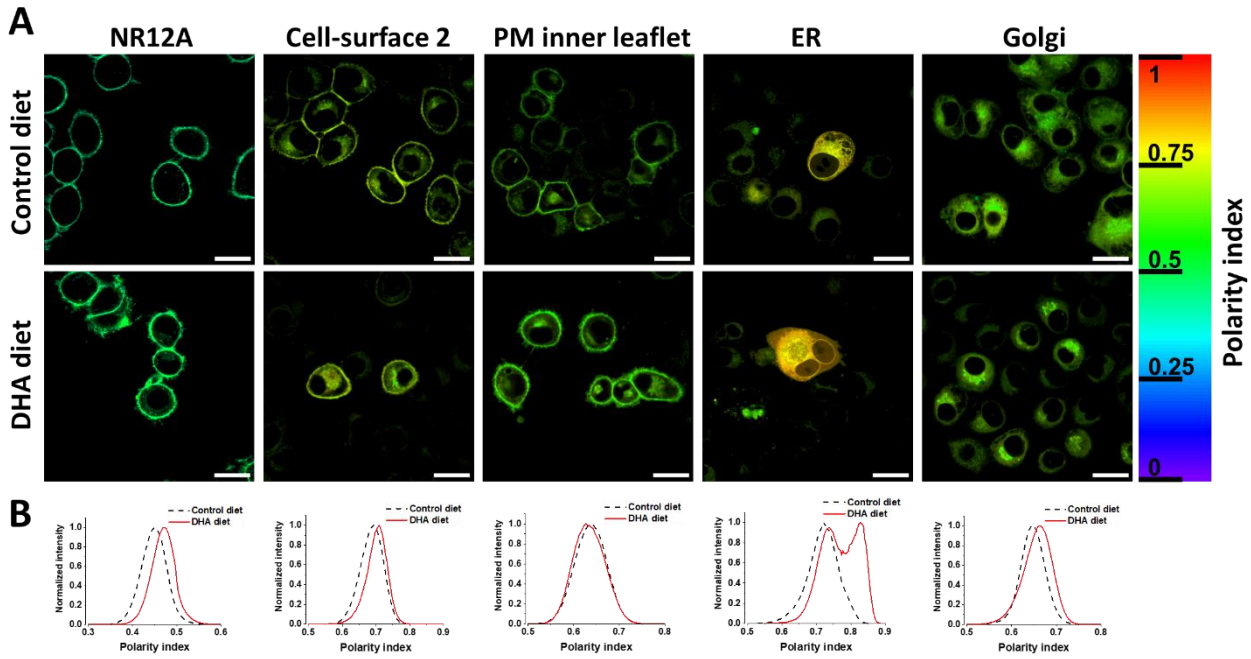

Figure S17. (A) Polarity imaging of transfected KB cells expressing HaloTagged proteins at various localization in CLSM with DHA diet. Scale bars: 20 µm. (B) Distribution curves of the polarity index normalized at their maximum.

Supplementary references

(1) Schneider, C. A.; Rasband, W. S.; Eliceiri, K. W. NIH Image to ImageJ: 25 years of image analysis, *Nat, Methods* **2012**, *9*, 671-675.
(2) Bolte, S.; Cordelieres, F. P. A guided tour into subcellular colocalization analysis in light microscopy, *J. Microsc.* **2006**, *224*, 213-232.
(3) Bachollet, S. P. J. T.; Shpinov, Y.; Broch, F.; Benaissa, H.; Gautier, A.; Pietrancosta, N.; Mallet, J.-M.; Dumat, B. An expanded palette of fluorogenic HaloTag probes with enhanced contrast for targeted cellular imaging, *Org. Biomol. Chem.* **2022**, *20*, 3619-3628.
(4) Plamont, M.-A.; Billon-Denis, E.; Maurin, S.; Gauron, C.; Pimenta, F. M.; Specht, C. G.; Shi, J.; Quérard, J.; Pan, B.; Rossignol, J.; Moncoq, K.; Morellet, N.; Volovitch, M.; Lescop, E.; Chen, Y.; Triller, A.; Vriz, S.; Le Saux, T.; Jullien, L.; Gautier, A. Small fluorescence-activating and absorption-shifting tag for tunable protein imaging in vivo, *Proc. Natl. Acad. Sci. U. S. A.* **2016**, *113*, 497-502.
(5) Danylchuk, D. I.; Moon, S.; Xu, K.; Klymchenko, A. S. Switchable Solvatochromic Probes for Live-Cell Super-resolution Imaging of Plasma Membrane Organization, *Angew. Chem. Int. Ed.* **2019**, *58*, 14920-14924.
(6) Neklesa, T. K.; Tae, H. S.; Schneekloth, A. R.; Stulberg, M. J.; Corson, T. W.; Sundberg, T. B.; Raina, K.; Holley, S. A.; Crews, C. M. Small-molecule hydrophobic tagging–induced degradation of HaloTag fusion proteins, *Nat, Chem, Biol,* **2011**, *7*, 538-543.
(7) Schneider, C. A.; Rasband, W. S.; Eliceiri, K. W. NIH Image to ImageJ: 25 years of image analysis, *Nat. Methods* **2012**, *9*, 671-675.
(8) Darwich, Z.; Kucherak, O. A.; Kreder, R.; Richert, L.; Vauchelles, R.; Mély, Y.; Klymchenko, A. S. Rational design of fluorescent membrane probes for apoptosis based on 3-hydroxyflavone, *Methods Appl. Fluoresc.* **2013**, *1*, 025002.
(9) Michelis, S.; Danglot, L.; Vauchelles, R.; Klymchenko, A. S.; Collot, M. Imaging and Measuring Vesicular Acidification with a Plasma Membrane-Targeted Ratiometric pH Probe, *Anal. Chem.* **2022**, *94*, 5996-6003.